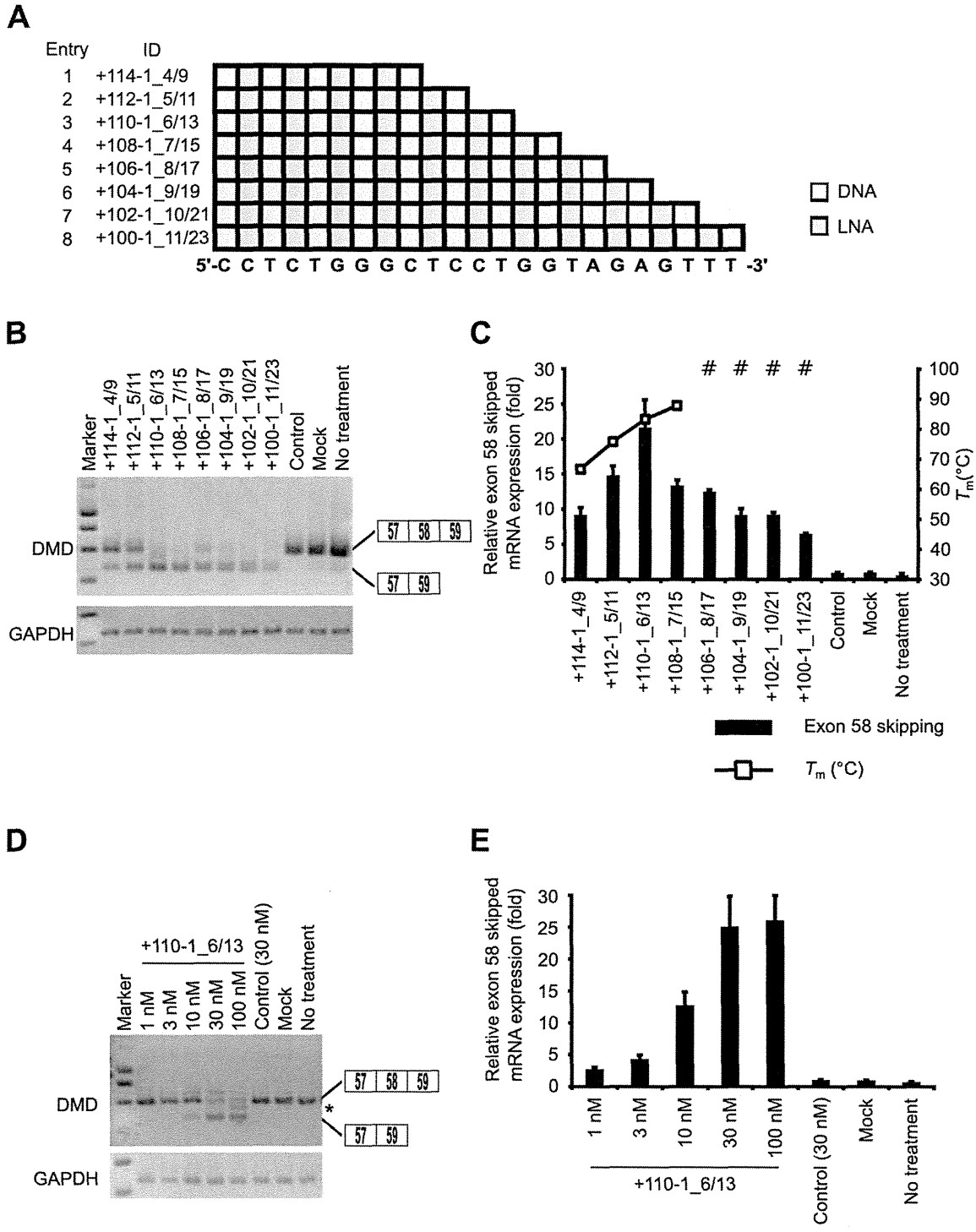

Figure 4. Comparison of the exon skipping activity of various lengths of LNA/DNA mixmer SSOs. (**A**) Schematic representation of the position of LNA in the SSOs used in this study. (**B** and **D**) The reporter cells were transfected with the indicated LNA/DNA mixmer SSOs (30 nM (B) or various concentrations (1–100 nM) (D)) for 24 h. RT-PCR analyses were performed as described in Figure 3B. The band marked by an asterisk represents a partial intron 58 inclusion product. (**C** and **E**) The levels of exon 58-skipped mRNA fragments were measured by quantitative real-time RT-PCR (for details see Materials and Methods and Figure 2G). Values represent the mean ± standard deviation of triplicate samples. Reproducible results were obtained from two independent experiments. The T_m of each SSO with a complementary RNA under low-sodium conditions is determined as described in Figure 3C. The data are the mean ± standard deviation ($n = 4$).

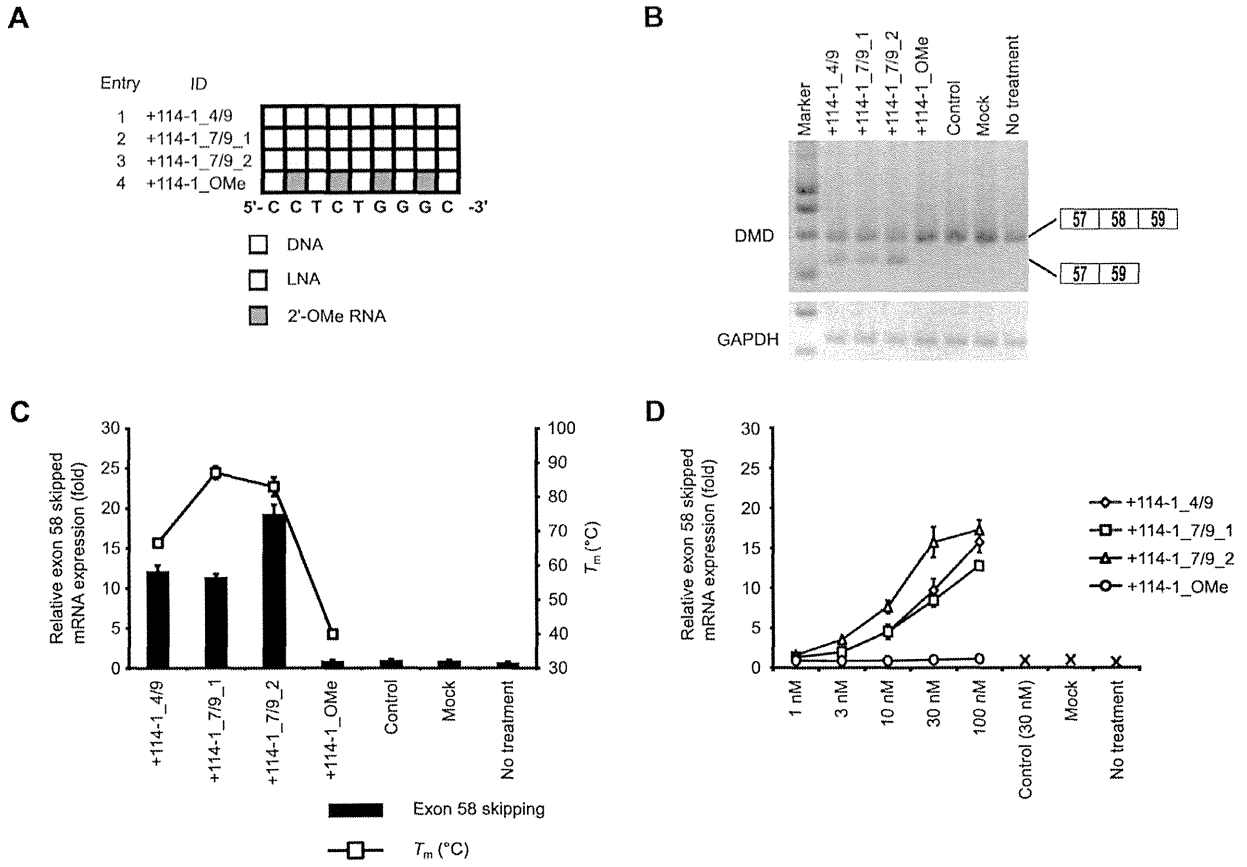

Figure 5. Exon skipping activity of 9-mer LNA/DNA mixmer SSOs. (**A**) Schematic representation of the position of LNA in the 9-mer SSOs used in this study. (**B**) The reporter cells were transfected with the indicated LNA/DNA mixmer SSOs (30 nM) for 24 h. RT-PCR analyses were performed as described in Figure 3B. (**C** and **D**) Quantitative real-time RT-PCR analyses of RNA samples from reporter cells treated with SSOs at 30 nM (C) or at various concentrations (1–100 nM) (D) for 24 h were performed as described in Figure 2G. Values represent the mean ± standard deviation of triplicate samples. Reproducible results were obtained from two independent experiments. The T_m of each SSO with a complementary RNA under low-sodium conditions is also shown. The data are the mean ± standard deviation ($n = 4$).

(+110-1_G117A, +110-1_G117C and +110-1_G117T), they can still induce exon skipping of exon 58. In contrast, mismatched LNA SSOs with two or three mismatches (+110-1_G115C/G117C and +110-1_G115C/g116c/G117C) did not show exon skipping activity. In the case of 9-mer LNA SSO (seven LNA and two DNA), one to three LNA mismatches abrogated the effect on exon 58 skipping. These results indicate that a 9-mer LNA SSO shows a better mismatch discrimination than a 13-mer LNA SSO. We next searched for target sequence of both 13- and 9-mer LNA SSOs using GGRNA (35). It is revealed that there were 914 genes that have perfect match with the 9-mer LNA SSO (+114-1_7/9_2). On the other hand, only 8 genes contain sequences perfectly matched to the 13-mer LNA SSO (+110-1_6/13) (Table 1). Thus, although 9-mer LNA SSOs improve mismatch discrimination in comparison with 13-mer LNA SSOs, 9-mer SSOs may be too short to target unique sites.

Induction of exon 58 skipping of endogenous human dystrophin transcript by using LNA SSO

Finally, to examine whether LNA SSOs modulate the splicing of endogenous human dystrophin transcript, we used primary HSMM cells. Cells were treated with the differentiation medium 24 h prior to transfection. Then, HSMM cells were transfected with 500 nM SSOs. Total RNA samples were prepared after a further 24 h incubation, and we assessed the expression of exon 58-skipped endogenous human dystrophin mRNA by means of RT-PCR. Although the 9-mer LNA SSO (+114-1_7/9_2) induced weak exon skipping, the 13-mer LNA SSO (+110-1_6/13) induced a high amount of exon skipping (Figure 8). In contrast, control SSO did not affected exon skipping. These data indicate that LNA SSOs are able to induce exon skipping of endogenous human dystrophin in cultured muscle cells.

DISCUSSION

In this study, we designed and evaluated the exon skipping ability of a series of LNA SSOs complementary to the hu-

Table 1. A number of genes that contain the sequence complementary to each AON. Sequences are shown from 5′ to 3′.

ID	Target sequence	Length (bp)	No. of genes containing the target sequence
+114-1_7/9_2	GCCCAGAGG	9	914
+110-1_6/13	AGGAGCCCAGAGG	13	8

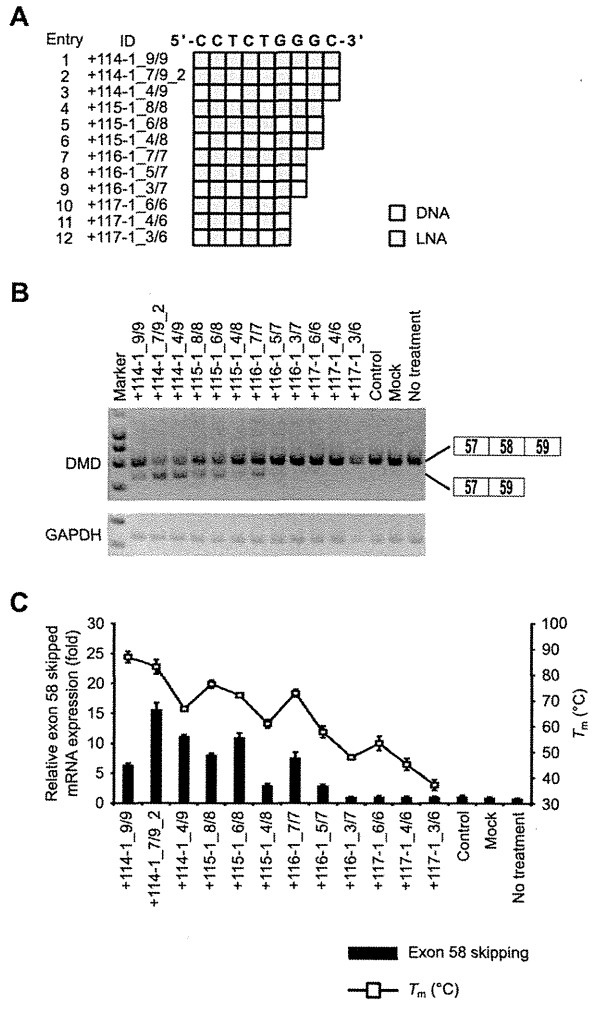

Figure 6. Comparison of exon skipping activity of short (6- to 9-mer) LNA SSOs. (**A**) Schematic representation of the position of LNA in the SSOs used in this study. (**B**) The reporter cells were transfected with the indicated LNA/DNA mixmer SSOs (30 nM) for 24 h. RT-PCR analyses were performed as described in Figure 3B. (**C**) The levels of exon 58-skipped mRNA fragments were measured by quantitative real-time RT-PCR (for details see Materials and Methods and Figure 2G). Values represent the mean ± standard deviation of triplicate samples. Reproducible results were obtained from two independent experiments. The T_m of each SSO with a complementary RNA under low-sodium conditions is also shown. The data are the mean ± standard deviation (n = 3–4).

man dystrophin exon 58 sequence. We also indicated that LNA SSOs induce endogenous dystrophin exon 58 skipping in primary human skeletal muscle cells.

To develop the splicing assay system we used native human dystrophin sequences because it is thought that the RNA structures play an important role in the regulation of splicing (39). According to previous reports, exon skipping target to exon 58 is applicable to only 0.1% of DMD patients (40). The average length of human dystrophin introns tends to be higher than 25 000 bp; therefore, the entire gene is inappropriate to introduce into a plasmid. However, intron 58, whose length is only 608 bp, has a much shorter sequence than other introns (41). We therefore selected exon 58 to construct our assay system despite the rarity of patients with mutations correctable by exon 58 skipping. On the other hand, the intron 57 sequence, consisting of 17 684 bp, is too long to insert into a reporter plasmid. Thus, although splicing regulatory sequences are located not only near exon–intron junctions but also intronic regions, we decided to use the human dystrophin minigene encompassing exons 57–59 by removing the sequence of intron 57 from position +207 to +17 486. Moreover, we established a stable Flp-In 293 cell line in which the reporter plasmid is incorporated into the genomic DNA, and that this screening cell line is easier to maintain than primary cells due to the robust growth. Because LNA SSOs selected by using this screeing cell line induced exon 58 skipping of endogenous dystrophin gene in the HSMM (Figure 8), this cell line is a useful evaluation tool for screening a lot of SSOs, as used in this study.

First, to identify effective SSOs capable of modulating exon skipping, 43 LNA SSOs, each with a length of 15 bases, were evaluated by RT-PCR. Exon skipping was induced at high levels by targeting either acceptor or donor sites with SSOs (Figure 2). In addition, this systematic screen also identified the 27-bp region from +70 to +96 of exon 58 as an appropriate target for SSOs. Interestingly, this region was predicted to be an ESE site by ESEfinder3.0 (Supplementary Figure S3) (37,38). This result was in agreement with previous studies using other chemically modified SSOs (42,43,44). Thus, splicing acceptor sites, splicing donor sites and ESE motifs are good targets for modulating exon splicing by LNA SSOs.

Second, we showed that exon skipping activity is dependent on the number of LNAs in the sequence of SSOs. Among the 15-mer mixmer SSOs, SSOs containing between five and eight LNA units showed especially high activity, and there was a correlation between their activity and the T_m of the SSOs with complementary RNA (Figure 3). In comparison to the LNA SSOs, the 2′-OMe SSO (five 2′-OMe and ten DNA) scarcely produced exon skipping (Figure 3), possibly because the exon skipping activity may be related to the binding affinity of each analogue. LNA-based oligonucleotides significantly enhanced hybridization to the complementary RNA, and the T_m was increased by 2°C–8°C for each LNA nucleotide incorporated (45,46), whereas

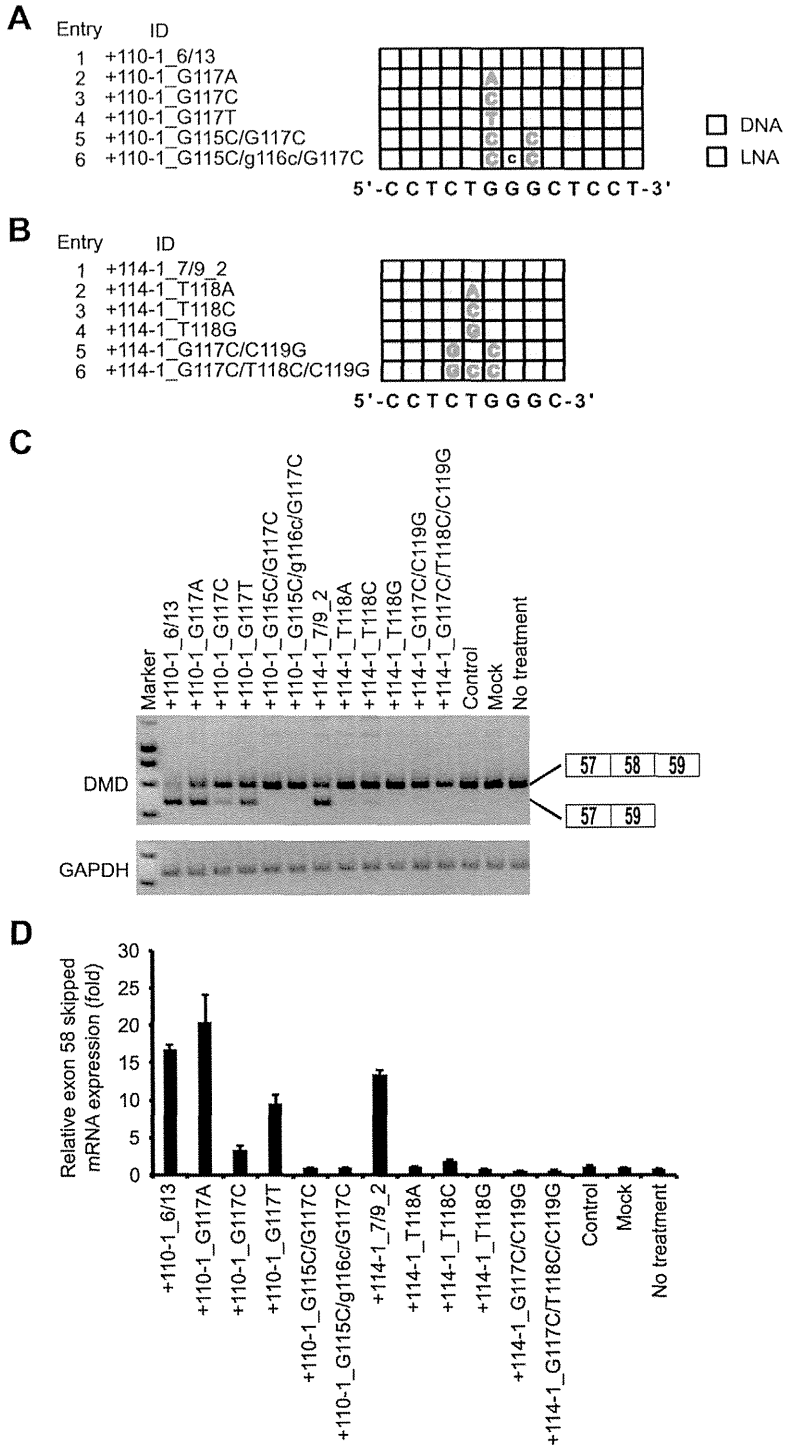

Figure 7. Assessment of specificity of LNA SSO. (**A** and **B**) Schematic representation of the position of LNA in the 13-mer SSOs (A) and the 9-mer SSOs (B) used in this study. The sequence in the box indicates a mismatch. Capital letter A, G, T: LNA; C: 5-methyl cytosine LNA; lowercase letter: DNA. (**C**) The reporter cells were transfected with the indicated LNA/DNA mixmer SSOs (30 nM) for 24 h. RT-PCR analyses were performed as described in Figure 3B. (**D**) The levels of exon 58-skipped mRNA fragments were measured by quantitative real-time RT-PCR (for details see Materials and Methods and Figure 2G). Values represent the mean ± standard deviation of triplicate samples. Reproducible results were obtained from two independent experiments.

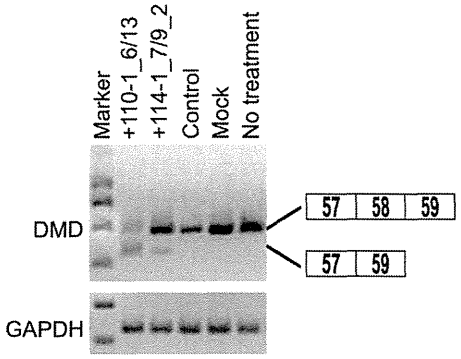

Figure 8. Exon skipping by LNA SSOs in primary human skeletal muscle cells. HSMM cells were transfected with the indicated LNA/DNA mixmer SSOs (500 nM) for 24 h. RT-PCR analyses show the full-length upper band (575 bp) and the skipped lower band (454 bp). LNA SSO (+10+24), which showed no exon skipping effects, was used as a control. GAPDH was used as an internal control.

the 2′-OMe modification resulted in an increase of only ~1°C per nucleotide incorporated (47). UV melting experiments performed under low-sodium conditions (10 mM phosphate buffer (pH 7.2) containing 10 mM NaCl) revealed that the T_m values of LNA SSO (five LNA and ten DNA) and 2′-OMe SSO (five 2′-OMe and ten DNA) were 69.5°C and 50.1°C, respectively (Supplementary Table S4). Thus, it seems that a higher melting temperature is associated with higher SSO activity. However, SSOs fully modified with LNA showed low activity despite their high T_m values. LNA-modified oligonucleotides often form stable self-structures (hairpin or self-dimer) (48). In particular, fully modified LNA SSOs might impair skipping activity because of self-dimerization, which led to decrease of effective SSO concentration for mRNA targeting (data not shown). In addition, we and others previously reported that AONs that possess very high binding affinity exhibit a relatively weak silencing ability (49,50). One of the reasons for this is that because AONs dissociated from the RNase H-dependent cleaved target mRNA could enter a new round of catalysis, LNA AONs with too high affinity might reduce the dissociation rate. Thus, LNA AONs are thought to require optimal binding affinity for efficient turnover activities in antisense reaction (51,52). Indeed, higher antisense effects were obtained by using LNA AONs whose T_m values were less than 65°C (10 mM phosphate buffer (pH 7.2) containing 100 mM NaCl) (49,50). In the case of exon skipping, SSO is also thought to be recycled after dissociation from the excised region (53). Thus, the values are different from those obtained for AONs, and there may be an optimum T_m range to design effective SSOs that incorporate LNA. To date, few studies have shown that LNA can be used in SSOs both *in vivo* and *in vitro* (17,18,19,20,21,22), and no information is available regarding the effects of the position and number of LNAs. Here, we report for the first time that SSOs fully modified with LNA have lower activity than LNA/DNA mixmer SSOs. This result may at least partially be explained by the optimization of T_m values described above and/or by the kinetics of duplex formation between LNA-based SSOs and RNA (54). Christensen reported that the rate of association of full-length LNA-based 10-mer oligonucleotides to complementary RNA was lower than that of a LNA/DNA mixmer (five LNA and five DNA) and the association constant of the full-length LNA-based oligonucleotide to complementary RNA was 1.5- to 2-fold less than that of the LNA/DNA mixmer in the presence of magnesium ions. Therefore, SSOs fully modified with LNA may be too rigid to use as splicing modulators, in contrast to LNA/DNA mixmers.

Third, our study of SSO length indicates that optimal lengths exist for LNA SSOs to modulate splicing. The quantitative real-time RT-PCR results indicated that the 13-mer SSO showed the highest effectiveness for exon skipping, whereas exon skipping activities of the above 15-mer LNA SSOs were decreased with increasing length (Figure 4). In this experiment, we used SSOs in which a LNA monomer was introduced on every other base. Therefore, longer SSOs exhibited higher binding abilities with smaller K_d values (Supplementary Table S6). These results are in good agreement with the T_m values. Thus, the decreased exon skipping activity should be brought by the other reason, such as intra- or intermolecular structures due to high number of LNAs in the SSO sequence (see above). On the other hand, in these experiments, all SSOs had a PS backbone in their sequence to provide nuclease resistance (55). Although the PS backbone decreases the T_m by ~1°C per substitution (56,57), the PS-LNA oligonucleotides have still high T_m values due to high affinity of LNA for the complementary RNA (Supplementary Tables S4 and S5) (58). Thus, PS backbone did not influence the binding affinity of PS-LNA SSO toward complementary RNA very much. Taken together, these ideas may explain why shorter LNA SSOs showed high splicing activity, and why 13-mer LNA/DNA SSO mixmers had the highest effectiveness for exon skipping.

Although Ittig *et al.* showed that a 9-mer fully modified LNA SSO has no significant exon skipping effect (20), we here demonstrated, for the first time, that LNA SSOs as short as 7 mers have the potential to modulate splicing in a concentration-dependent manner provided that they are highly modified and display high T_m values (Figures 5 and 6). Shorter SSOs may have a further advantage in that the production costs of oligonucleotide drugs are higher than that of small molecules; therefore, shorter oligonucleotides may provide a cost-effective solution to the development of oligonucleotide drugs. Although, the activity of the 9-mer SSO (four LNA and five DNA) was weaker than that of the 13-mer SSO, quantitative real-time RT-PCR experiments revealed that the expression of skipped mRNA was similar among 9-, 19-, 21- and 23-mer SSOs (Figure 4). Intriguingly, when we compared two 9-mer LNA/DNA mixmer SSOs containing seven LNA analogues at different positions in each sequence, one of them presented 1.5-fold higher activity than the other despite their similar T_m values (87.1°C and 83.1°C) (Supplementary Table S7). Thus, the position of LNA analogues in the SSO sequence may be an important factor for exon skipping. Of note, the 9-mer 2′-OMe SSO (four 2′-OMe and five DNA), which has a low T_m value (40.0°C), exhibited no exon skipping activity at all (Figure 5).

Kandimalla *et al.* reported that short oligonucleotides (9-mers) bind more specifically than longer oligonucleotides (such as 21-mers), possibly because longer oligonucleotides have a higher chance of binding to various target sequences containing up to two mismatches than do short oligonucleotides, given the sufficient T_m values of longer oligonucleotides for forming duplexes with mismatched sequences (59). Indeed, Guterstam *et al.* demonstrated that the 18-mer PS LNA/2'-OMe mixmers with four mismatches, including one LNA mismatch, induced exon skipping (17). On the other hand, Obad *et al.* reported that 8-mer LNAs, termed tiny LNAs, inhibit microRNA activity without off-target effects (60). In this study, we evaluated the sequence specificity of LNA/DNA mixmer SSOs by introducing mismatches. The 13-mer LNA SSO (+110-1_6/13) containing one LNA mismatch was able to induce exon skipping, while the exon skipping activity is abolished when one to three LNA mismatches are introduced in the center of the 9-mer LNA SSO (+114-1_7/9_2). Thus, the 9-mer LNA SSO improved mismatch discrimination in comparison with the 13-mer LNA SSO. However, in our *in silico* analysis, the number of target genes that have perfect match with 9-mer LNA SSO (+114-1_7/9_2) is far larger than that of the 13-mer LNA SSO (+110-1_6/13) (914 genes and 8 genes, respectively) (Table 1). Although the ability to discriminate between the matched and mismatched sequences is improved by shorter SSO, these results suggest that it is important to design LNA SSOs in consideration of off target-effects.

In conclusion, we found that the number of LNAs in the SSO sequence, the T_m of the SSOs and the length of the LNA SSOs are key factors for their activity. We also show for the first time that 7-mer LNA SSOs induce exon skipping. Our findings suggest that LNA SSO-mediated exon skipping may be an attractive therapeutic strategy for genetic diseases.

SUPPLEMENTARY DATA

Supplementary Data are available at NAR Online.

FUNDING

Grant-in-Aid for Exploratory Research and Project MEET, Osaka University Graduate School of Medicine. Funding for open access charge: Grant-in-Aid for Scientific Research (A).

Conflict of interest statement. None declared.

REFERENCES

1. Modrek,B. and Lee,C. (2002) A genomic view of alternative splicing. *Nat. Genet.*, **30**, 13–19.
2. Perez,B., Rincon,A., Jorge-Finnigan,A., Richard,E., Merinero,B., Ugarte,M. and Desviat,L.R. (2009) Pseudoexon exclusion by antisense therapy in methylmalonic aciduria (MMAuria). *Hum. Mutat.*, **30**, 1676–1682.
3. Cartegni,L., Chew,S.L. and Krainer,A.R. (2002) Listening to silence and understanding nonsense: exonic mutations that affect splicing. *Nat. Rev. Genet.*, **3**, 285–298.
4. Padgett,R.A. (2012) New connections between splicing and human disease. *Trends Genet.*, **28**, 147–154.
5. Hammond,S.M. and Wood,M.J. (2011) Genetic therapies for RNA mis-splicing diseases. *Trends Genet.*, **27**, 196–205.
6. Spitali,P. and Aartsma-Rus,A. (2012) Splice modulating therapies for human disease. *Cell*, **148**, 1085–1088.
7. Wahl,M.C., Will,C.L. and Luhrmann,R. (2009) The spliceosome: design principles of a dynamic RNP machine. *Cell*, **136**, 701–718.
8. Kole,R., Krainer,A.R. and Altman,S. (2012) RNA therapeutics: beyond RNA interference and antisense oligonucleotides. *Nat. Rev. Drug Discov.*, **11**, 125–140.
9. Dominski,Z. and Kole,R. (1993) Restoration of correct splicing in thalassemic pre-mRNA by antisense oligonucleotides. *Proc. Natl. Acad. Sci. U. S. A.*, **90**, 8673–8677.
10. Saleh,A.F., Arzumanov,A.A. and Gait,M.J. (2012) Overview of alternative oligonucleotide chemistries for exon skipping. *Methods Mol. Biol.*, **867**, 365–378.
11. Yamamoto,T., Nakatani,M., Narukawa,K. and Obika,S. (2011) Antisense drug discovery and development. *Future Med. Chem.*, **3**, 339–365.
12. Singh,S.K., Nielsen,P., Koshkin,A.A. and Wengel,J. (1998) LNA (locked nucleic acids): synthesis and high-affinity nucleic acid recognition. *Chem. Commun.*, **4**, 455–456.
13. Obika,S., Nanbu,D., Hari,Y., Morio,K., In,Y., Ishida,T. and Imanishi,T. (1997) Synthesis of 2'-O,4'-C-methyleneuridine and -cytidine. Novel bicyclic nucleosides having a fixed C-3,-endo sugar puckering. *Tetrahedron Lett.*, **38**, 8735–8738.
14. Braasch,D.A. and Corey,D.R. (2001) Locked nucleic acid (LNA): fine-tuning the recognition of DNA and RNA. *Chem. Biol.*, **8**, 1–7.
15. Bondensgaard,K., Petersen,M., Singh,S.K., Rajwanshi,V.K., Kumar,R., Wengel,J. and Jacobsen,J.P. (2000) Structural studies of LNA:RNA duplexes by NMR: conformations and implications for RNase H activity. *Chemistry*, **6**, 2687–2695.
16. Vester,B. and Wengel,J. (2004) LNA (locked nucleic acid): high-affinity targeting of complementary RNA and DNA. *Biochemistry*, **43**, 13233–13241.
17. Guterstam,P., Lindgren,M., Johansson,H., Tedebark,U., Wengel,J., El Andaloussi,S. and Langel,U. (2008) Splice-switching efficiency and specificity for oligonucleotides with locked nucleic acid monomers. *Biochem. J.*, **412**, 307–313.
18. Aartsma-Rus,A., Kaman,W.E., Bremmer-Bout,M., Janson,A.A., den Dunnen,J.T., van Ommen,G.J. and van Deutekom,J.C. (2004) Comparative analysis of antisense oligonucleotide analogs for targeted DMD exon 46 skipping in muscle cells. *Gene Ther.*, **11**, 1391–1398.
19. Graziewicz,M.A., Tarrant,T.K., Buckley,B., Roberts,J., Fulton,L., Hansen,H., Orum,H., Kole,R. and Sazani,P. (2008) An endogenous TNF-alpha antagonist induced by splice-switching oligonucleotides reduces inflammation in hepatitis and arthritis mouse models. *Mol. Ther.*, **16**, 1316–1322.
20. Ittig,D., Liu,S., Renneberg,D., Schumperli,D. and Leumann,C.J. (2004) Nuclear antisense effects in cyclophilin A pre-mRNA splicing by oligonucleotides: a comparison of tricyclo-DNA with LNA. *Nucleic Acids Res.*, **32**, 346–353.
21. Roberts,J., Palma,E., Sazani,P., Orum,H., Cho,M. and Kole,R. (2006) Efficient and persistent splice switching by systemically delivered LNA oligonucleotides in mice. *Mol. Ther.*, **14**, 471–475.
22. Yilmaz-Elis,A.S., Aartsma-Rus,A., t Hoen,P.A., Safdar,H., Breukel,C., van Vlijmen,B.J., van Deutekom,J., de Kimpe,S., van Ommen,G.J. and Verbeek,J.S. (2013) Inhibition of IL-1 Signaling by antisense oligonucleotide-mediated exon skipping of IL-1 receptor accessory protein (IL-1RAcP). *Mol. Ther. Nucleic Acids*, **2**, e66.
23. Goemans,N.M., Tulinius,M., van den Akker,J.T., Burm,B.E., Ekhart,P.F., Heuvelmans,N., Holling,T., Janson,A.A., Platenburg,G.J., Sipkens,J.A. *et al.* (2011) Systemic administration of PRO051 in Duchenne's muscular dystrophy. *N. Engl. J. Med.*, **364**, 1513–1522.
24. van Deutekom,J.C., Janson,A.A., Ginjaar,I.B., Frankhuizen,W.S., Aartsma-Rus,A., Bremmer-Bout,M., den Dunnen,J.T., Koop,K., van der Kooi,A.J., Goemans,N.M. *et al.* (2007) Local dystrophin restoration with antisense oligonucleotide PRO051. *N. Engl. J. Med.*, **357**, 2677–2686.
25. Morita,K., Hasegawa,C., Kaneko,M., Tsutsumi,S., Sone,J., Ishikawa,T., Imanishi,T. and Koizumi,M. (2002) 2'-O,4'-C-ethylene-bridged nucleic acids (ENA): highly nuclease-resistant and thermodynamically stable oligonucleotides for antisense drug. *Bioorg. Med. Chem. Lett.*, **12**, 73–76.

26. Cirak,S., Arechavala-Gomeza,V., Guglieri,M., Feng,L., Torelli,S., Anthony,K., Abbs,S., Garralda,M.E., Bourke,J., Wells,D.J. *et al.* (2011) Exon skipping and dystrophin restoration in patients with Duchenne muscular dystrophy after systemic phosphorodiamidate morpholino oligomer treatment: an open-label, phase 2, dose-escalation study. *Lancet*, **378**, 595–605.
27. Kinali,M., Arechavala-Gomeza,V., Feng,L., Cirak,S., Hunt,D., Adkin,C., Guglieri,M., Ashton,E., Abbs,S., Nihoyannopoulos,P. *et al.* (2009) Local restoration of dystrophin expression with the morpholino oligomer AVI-4658 in Duchenne muscular dystrophy: a single-blind, placebo-controlled, dose-escalation, proof-of-concept study. *Lancet Neurol.*, **8**, 918–928.
28. Mendell,J.R., Rodino-Klapac,L.R., Sahenk,Z., Roush,K., Bird,L., Lowes,L.P., Alfano,L., Gomez,A.M., Lewis,S., Kota,J. *et al.* (2013) Eteplirsen for the treatment of Duchenne muscular dystrophy. *Ann. Neurol.*, **74**, 637–647.
29. Muntoni,F. and Wood,M.J. (2011) Targeting RNA to treat neuromuscular disease. *Nat. Rev. Drug Discov.*, **10**, 621–637.
30. Aartsma-Rus,A. (2012) Overview on AON design. *Methods Mol. Biol.*, **867**, 117–129.
31. Aartsma-Rus,A., van Vliet,L., Hirschi,M., Janson,A.A., Heemskerk,H., de Winter,C.L., de Kimpe,S., van Deutekom,J.C., t Hoen,P.A. and van Ommen,G.J. (2009) Guidelines for antisense oligonucleotide design and insight into splice-modulating mechanisms. *Mol. Ther.*, **17**, 548–553.
32. Orengo,J.P., Bundman,D. and Cooper,T.A. (2006) A bichromatic fluorescent reporter for cell-based screens of alternative splicing. *Nucleic Acids Res.*, **34**, e148.
33. Rozen,S. and Skaletsky,H. (2000) Primer3 on the WWW for general users and for biologist programmers. *Methods Mol. Biol.*, **132**, 365–386.
34. Wu,B., Benrashid,E., Lu,P., Cloer,C., Zillmer,A., Shaban,M. and Lu,Q.L. (2011) Targeted skipping of human dystrophin exons in transgenic mouse model systemically for antisense drug development. *PLoS One*, **6**, e19906.
35. Naito,Y. and Bono,H. (2012) GGRNA: an ultrafast, transcript-oriented search engine for genes and transcripts. *Nucleic Acids Res.*, **40**, W592–W596.
36. Kurreck,J., Wyszko,E., Gillen,C. and Erdmann,V.A. (2002) Design of antisense oligonucleotides stabilized by locked nucleic acids. *Nucleic Acids Res.*, **30**, 1911–1918.
37. Cartegni,L., Wang,J., Zhu,Z., Zhang,M.Q. and Krainer,A.R. (2003) ESEfinder: a web resource to identify exonic splicing enhancers. *Nucleic Acids Res.*, **31**, 3568–3571.
38. Smith,P.J., Zhang,C., Wang,J., Chew,S.L., Zhang,M.Q. and Krainer,A.R. (2006) An increased specificity score matrix for the prediction of SF2/ASF-specific exonic splicing enhancers. *Hum. Mol. Genet.*, **15**, 2490–2508.
39. Warf,M.B. and Berglund,J.A. (2009) Role of RNA structure in regulating pre-mRNA splicing. *Trends Biochem. Sci.*, **35**, 169–178.
40. Aartsma-Rus,A., Fokkema,I., Verschuuren,J., Ginjaar,I., van Deutekom,J., van Ommen,G.J. and den Dunnen,J.T. (2009) Theoretic applicability of antisense-mediated exon skipping for Duchenne muscular dystrophy mutations. *Hum. Mutat.*, **30**, 293–299.
41. Pozzoli,U., Elgar,G., Cagliani,R., Riva,L., Comi,G.P., Bresolin,N., Bardoni,A. and Sironi,M. (2003) Comparative analysis of vertebrate dystrophin loci indicate intron gigantism as a common feature. *Genome Res.*, **13**, 764–772.
42. Wilton,S.D., Fall,A.M., Harding,P.L., McClorey,G., Coleman,C. and Fletcher,S. (2007) Antisense oligonucleotide-induced exon skipping across the human dystrophin gene transcript. *Mol. Ther.*, **15**, 1288–1296.
43. Aartsma-Rus,A., De Winter,C.L., Janson,A.A., Kaman,W.E., Van Ommen,G.J., Den Dunnen,J.T. and Van Deutekom,J.C. (2005) Functional analysis of 114 exon-internal AONs for targeted DMD exon skipping: indication for steric hindrance of SR protein binding sites. *Oligonucleotides*, **15**, 284–297.
44. Aartsma-Rus,A., Houlleberghs,H., van Deutekom,J.C., van Ommen,G.J. and t Hoen,P.A. (2010) Exonic sequences provide better targets for antisense oligonucleotides than splice site sequences in the modulation of Duchenne muscular dystrophy splicing. *Oligonucleotides*, **20**, 69–77.
45. Koshkin,A.A., Singh,S.K., Nielsen,P., Rajwanshi,V.K., Kumar,R., Meldgaard,M., Olsen,C.E. and Wengel,J. (1998) LNA (Locked Nucleic Acids): synthesis of the adenine, cytosine, guanine, 5-methylcytosine, thymine and uracil bicyclonucleoside monomers, oligomerisation, and unprecedented nucleic acid recognition. *Tetrahedron*, **54**, 3607–3630.
46. Obika,S., Nanbu,D., Hari,Y., Andoh,J., Morio,K., Doi,T. and Imanishi,T. (1998) Stability and structural features of the duplexes containing nucleoside analogues with a fixed N-type conformation, 2 '-O,4 '-C-methyleneribonucleosides. *Tetrahedron Lett.*, **39**, 5401–5404.
47. Lesnik,E.A., Guinosso,C.J., Kawasaki,A.M., Sasmor,H., Zounes,M., Cummins,L.L., Ecker,D.J., Cook,P.D. and Freier,S.M. (1993) Oligodeoxynucleotides containing 2'-O-modified adenosine: synthesis and effects on stability of DNA:RNA duplexes. *Biochemistry*, **32**, 7832–7838.
48. Lennox,K.A. and Behlke,M.A. (2011) Chemical modification and design of anti-miRNA oligonucleotides. *Gene Ther.*, **18**, 1111–1120.
49. Yamamoto,T., Yasuhara,H., Wada,F., Harada-Shiba,M., Imanishi,T. and Obika,S. (2012) Superior silencing by 2',4'-BNA(NC)-based short antisense oligonucleotides compared to 2',4'-BNA/LNA-based apolipoprotein B antisense inhibitors. *J. Nucleic Acids*, **2012**, 707323.
50. Straarup,E.M., Fisker,N., Hedtjarn,M., Lindholm,M.W., Rosenbohm,C., Aarup,V., Hansen,H.F., Orum,H., Hansen,J.B. and Koch,T. (2010) Short locked nucleic acid antisense oligonucleotides potently reduce apolipoprotein B mRNA and serum cholesterol in mice and non-human primates. *Nucleic Acids Res.*, **38**, 7100–7111.
51. Yamamoto,T., Fujii,N., Yasuhara,H., Wada,S., Wada,F., Shigesada,N., Harada-Shiba,M. and Obika,S. (2014) Evaluation of multiple-turnover capability of locked nucleic acid antisense oligonucleotides in cell-free RNase H-mediated antisense reaction and in mice. *Nucleic Acid Ther.*, 10.1089/nat.2013.0470.
52. Pedersen,L., Hagedorn,P.H., Lindholm,M.W. and Lindow,M. (2014) A kinetic model explains why shorter and less affine enzyme-recruiting oligonucleotides can be more potent. *Mol. Ther. Nucleic Acids*, **3**, e149.
53. Sierakowska,H., Sambade,M.J., Agrawal,S. and Kole,R. (1996) Repair of thalassemic human beta-globin mRNA in mammalian cells by antisense oligonucleotides. *Proc. Natl. Acad. Sci. U. S. A.*, **93**, 12840–12844.
54. Christensen,U. (2007) Thermodynamic and kinetic characterization of duplex formation between 2'-O, 4'-C-methylene-modified oligoribonucleotides, DNA and RNA. *Biosci. Rep.*, **27**, 327–333.
55. Akhtar,S., Kole,R. and Juliano,R.L. (1991) Stability of antisense DNA oligodeoxynucleotide analogs in cellular extracts and sera. *Life Sci.*, **49**, 1793–1801.
56. Stein,C.A., Subasinghe,C., Shinozuka,K. and Cohen,J.S. (1988) Physicochemical properties of phosphorothioate oligodeoxynucleotides. *Nucleic Acids Res.*, **16**, 3209–3221.
57. Freier,S.M. and Altmann,K.H. (1997) The ups and downs of nucleic acid duplex stability: structure-stability studies on chemically-modified DNA:RNA duplexes. *Nucleic Acids Res.*, **25**, 4429–4443.
58. Kumar,R., Singh,S.K., Koshkin,A.A., Rajwanshi,V.K., Meldgaard,M. and Wengel,J. (1998) The first analogues of LNA (locked nucleic acids): phosphorothioate-LNA and 2'-thio-LNA. *Bioorg. Med. Chem. Lett.*, **8**, 2219–2222.
59. Kandimalla,E.R., Manning,A., Lathan,C., Byrn,R.A. and Agrawal,S. (1995) Design, biochemical, biophysical and biological properties of cooperative antisense oligonucleotides. *Nucleic Acids Res.*, **23**, 3578–3584.
60. Obad,S., dos Santos,C.O., Petri,A., Heidenblad,M., Broom,O., Ruse,C., Fu,C., Lindow,M., Stenvang,J., Straarup,E.M. *et al.* (2011) Silencing of microRNA families by seed-targeting tiny LNAs. *Nat. Genet.*, **43**, 371–378.

[Supplementary Data]

Design and evaluation of locked nucleic acid-based splice-switching oligonucleotides in vitro

Takenori Shimo[1], Keisuke Tachibana[1], Kiwamu Saito[1], Tokuyuki Yoshida[1,2], Erisa Tomita[3], Reiko Waki[1], Tsuyoshi Yamamoto[1], Takefumi Doi[1], Takao Inoue[1,2], Junji Kawakami[3,4] and Satoshi Obika[1,*]

[1] Graduate School of Pharmaceutical Sciences, Osaka University, 1-6, Yamadaoka, Suita, Osaka, 565-0871, Japan
[2] Division of Cellular and Gene Therapy Products, National Institute of Health Sciences, 1-18-1 Kamiyoga, Setagaya-ku, Tokyo 158-8501, Japan
[3] Department of Nanobiochemistry, FIRST, Konan University, 7-1-20 Minatojima-minamimachi, Chuo-ku, Kobe 650-0047, Japan
[4] Frontier Institute for Biomolecular Engineering Research (FIBER), Konan University, 7-1-20 Minatojima-minamimachi, Chuo-ku, Kobe 650-0047, Japan

* To whom correspondence should be addressed. Tel: +81 6 6879 8200; Fax: +81 6 6879 8204; Email: obika@phs.osaka-u.ac.jp

The authors wish it to be known that, in their opinion, the first two authors should be regarded as joint First Authors.

SUPPLEMENTARY MATERIAL AND METHODS

Thermodynamic analysis of various lengths of LNA/DNA mixmer SSOs duplexes

Gibbs free energy change ($\Delta G°_{25}$) during the duplex formation of 9-mer SSO (+114-1_4/9) and the complementary RNA was calculated by standard thermal UV melting analysis (61). Dissociation constant (K_d) for the duplex was determined using the equation, $K_d = 1/\exp(-\Delta G°/298.15R)$, where R was gas constant. Because the binding of our LNA/DNA mixmer SSOs to mRNA was too strong to determine the dissociation constant directly from calorimetric or stopped flow experiments, $\Delta G°_{25}$ and dissociation constant at 25°C for the other SSOs were estimated by competition assays.

In our analysis, equal amount of a 5′ 6-carboxyfluorescein (6-FAM)-labeled SSO (A strand) and the complementary RNA (B strand) was mixed with various amount of a competitor SSO (X strand) in 10 mM phosphate buffer (pH 7.2) containing 100 mM NaCl. The initial concentration of each (A and B) strand was C_0 (6.67×10^{-8} M). To give equal opportunities to the competing strands (A and X) for hybridization with RNA (B strand), B strand was added to the solution in last. The solution was heated to 100°C and annealed to 25°C with cooling rate 0.5°C/min. After separation by 15% non-denaturing PAGE, the gel was analyzed using an ImageQuant LAS4010 (GE Healthcare Bio-sciences AB, Uppsala, Sweden). The fluorescence intensity that corresponds to the amount of a labeled duplex (F_{AB}) was measured by using ImageJ software. The decrement of the F_{AB} with increasing free competitor SSO concentration [X] was fitted to the following equation with an assumption [A] >> $K_{d(AB)}$, where Max and BG respectively indicated maximum change of F_{AB} and background fluorescence intensity, and half maximal inhibitory concentration of the competitor SSO (IC_{50}) was determined (Supplementary Figure S11).

$$F_{AB} = Max(1 - [X]/([X] + IC_{50})) + BG$$

In this analysis, IC_{50} is defined as the concentration of free competitor SSO at which half of the labeled duplex is present at equilibrium. The analysis was carried out at least three times independently and the average IC_{50} values were adopted. The relative affinities between two competing molecules were calculated as follows.

$$K_{d(BX)}/K_{d(AB)} = 2 \times IC_{50}/C_0$$

$$\Delta\Delta G°_{25} = \Delta G°_{25(BX)} - \Delta G°_{25(AB)} = 298.15R \ln(K_{d(BX)}/K_{d(AB)})$$

Based on the resulting $\Delta\Delta G°_{25}$ and actual measured $\Delta G°_{25}$ value for 9-mer SSO (+114-1_4/9), $\Delta G°_{25}$ and K_d values for the other SSOs were estimated.

SUPPLEMENTARY TABLE AND FIGURES LEGENDS

Supplementary Table S1. SSOs used for the first screening. Nine SSOs for dystrophin exon 58 skipping are shown. Sequences are shown from 5' to 3'. Capital letter A, G, T: LNA; C: 5-methyl cytosine LNA; lowercase letter: DNA.

Supplementary Table S2. SSOs used for the second screening. Twenty-nine SSOs for dystrophin exon 58 skipping are shown. Sequences are shown from 5' to 3'.

Supplementary Table S3. SSOs used for the third screening. Ten SSOs for dystrophin exon 58 skipping are shown. Sequences are shown from 5' to 3'.

Supplementary Table S4. SSOs targeting 5' splice site used for T_m and exon skipping analysis. SSOs for each experiment are shown. Sequences are shown from 5' to 3'. T_m values (low salt: 2 μM duplex in 10 mM phosphate buffer (pH 7.2), 10 mM NaCl (n = 4); medium salt: 2 μM duplex in 10 mM phosphate buffer (pH 7.2), 100 mM NaCl (n = 3)) were determined (± SD). Capital letter A, G, T: LNA; C: 5-methyl cytosine LNA; capital letter with underline: 2'-OMe RNA; lowercase letter: DNA.

Supplementary Table S5. SSOs targeting 3' splice site used for T_m and exon skipping analysis. SSOs for each experiment are shown. Sequences are shown from 5' to 3'. T_m values (2 μM duplex in 10 mM phosphate buffer (pH 7.2), 10 mM NaCl) were determined in four independent experiments (± SD).

Supplementary Table S6. SSOs used for analysis of SSO length. SSOs for each experiment are shown. Sequences are shown from 5' to 3'. T_m values (2 μM duplex in 10 mM phosphate buffer (pH 7.2), 10 mM NaCl) were determined in four independent experiments (± SD). Gibbs free energy change ($\Delta G°_{25}$) for SSO (+114-1_4/9) was calculated by standard thermal UV melting analysis (2 μM duplex in 10 mM phosphate buffer (pH 7.2), 100 mM NaCl). Dissociation constant (K_d) for SSO (+114-

1_4/9) was calculated using the equation: K_d = 1/exp(-$\Delta G°$/298.15R). $\Delta G°_{25}$ and K_d for the other SSOs were estimated by competition assays.

Supplementary Table S7. SSOs used for analysis of 9-mer SSOs. SSOs for each experiment are shown. Sequences are shown from 5' to 3'. T_m values (2 μM duplex in 10 mM phosphate buffer (pH 7.2), 10 mM NaCl) were determined in four independent experiments (± SD).

Supplementary Table S8. SSOs used for analysis of short SSOs. SSOs for each experiment are shown. Sequences are shown from 5' to 3'. T_m values (2 μM duplex in 10 mM phosphate buffer (pH 7.2), 10 mM NaCl) were determined in three or four independent experiments (± SD).

Supplementary Table S9. SSOs used for mismatch discrimination. SSOs for each experiment are shown. Sequences are shown from 5' to 3'. Nucleotides of mismatch sites are double underlined.

Supplementary Table S10. Primers used for RT-PCR analysis. Sequences of forward (For.) and reverse (Rev.) primer for each target are shown. Sequences are shown from 5' to 3'.

Supplementary Table S11. Primers used for quantitative real-time RT-PCR analysis. Sequences of forward (For.) and reverse (Rev.) primer for each target are shown. Sequences are shown from 5' to 3'.

Supplementary Figure S1. Schematic representation of the dystrophin reporter minigene and of the its splicing pattern. Human dystrophin exons are indicated by open boxes and introns by narrow lines. Solid boxes represent vector sequences. Lines connecting the exons represent the splicing patterns. The expected mRNA structures, indicated below the minigene structure result from inclusion or exclusion of exon 58. Small black arrows and small purple arrows indicate approximate positions of primers used for RT-PCR and quantitative real-time RT-PCR, respectively.

Supplementary Figure S2. Screening of LNA SSOs designed to induce dystrophin exon 58 skipping. **(A, B)** Reporter cells were transfected with the indicated SSOs (100 nM) for 24 h. The levels of reporter minigene mRNA fragments were measured by RT-PCR, and the signal intensity of each band was normalized according to its nucleotide composition. The exon skipping percentage was calculated as the amount of exon skipped transcript relative to the total amount of exon skipped and full-length transcripts. Values represent the mean ± standard deviation of triplicate or sixplicate samples. Reproducible results were obtained from two independent experiments. (A) and (B) express the results of the first and the second screening, respectively. Mock: treated with Lipofectamine only; no treatment: no transfection.

Supplementary Figure S3. Prediction of splice factor binding site in human dystrophin exon 58. The locations of potential binding sites for the splicing factors SRSF1 (SF2/ASF), SRSF1 (IgM-BRCA1), SRSF2 (SC35), SRSF5 (SRp40), and SRSF6 (SRp55) in human dystrophin exon 58 and 50 bases of flanking intronic sequence were predicted by using ESEfinder3.0.

Supplementary Figure S4. Effect of the number of LNA variations on exon skipping activity. **(A, B)** Reporter cells were transfected with the indicated SSOs (30 nM), targeting the 5' (A) or 3' (B) splice site, for 24 h. The levels of reporter minigene mRNA fragments were measured by RT-PCR, and the signal intensity of each band was normalized according to its nucleotide composition. The exon skipping percentage was calculated as the amount of exon skipped transcript relative to the total amount of exon skipped and full-length transcripts. LNA SSO (+10+24), which showed no exon skipping effects, was used as a control. Values represent the mean ± standard deviation of triplicate samples. Reproducible results were obtained from two independent experiments. The T_m of each SSO with a complementary RNA under low-sodium conditions is also shown. # indicates that no sigmoidal melting curve was observed, even at higher T_m values. The data are the mean ± standard deviation (n = 4). Mock: treated with Lipofectamine only; no treatment: no transfection.

Supplementary Figure S5. Assessment of the effect of the length of LNA/DNA mixmer SSOs on exon skipping. Reporter cells were transfected with the indicated SSOs (30 nM) for 24 h. The levels of reporter minigene mRNA fragments were measured by RT-PCR, and the signal intensity of each band was normalized according to its nucleotide composition. The exon skipping percentage was calculated as the amount of exon skipped transcript relative to the total amount of exon skipped and full-length transcripts. LNA SSO (+10+24), which showed no exon skipping effects, was used as a control. Values represent the mean ± standard deviation of triplicate samples. Reproducible results were obtained from two independent experiments. The T_m of each SSO with a complementary RNA under low-sodium conditions is also shown. # indicates that no sigmoidal melting curve was observed, even at higher T_m values. The data are the mean ± standard deviation (n = 4). Mock: treated with Lipofectamine only; no treatment: no transfection.

Supplementary Figure S6. Exon skipping activity of LNA/DNA mixmer SSOs at various concentrations. **(A, C)** Reporter cells were transfected with the indicated SSOs, targeting the 3' (A) or 5' (C) splice site, at various concentrations for 24 h. The levels of reporter minigene mRNA fragments were measured by RT-PCR, and the signal intensity of each band was normalized according to its nucleotide composition. The exon skipping percentage was calculated as the amount of exon skipped transcript relative to the total amount of exon skipped and full-length transcripts. LNA SSO (+10+24), which showed no exon skipping effects, was used as a control. **(B)** RT-PCR analysis shows the full-length upper band (587 bp) and the skipped lower band (466 bp). GAPDH was used as an internal control. **(D)** The exon 58 skipping levels were measured by quantitative real-time RT-PCR and normalized to GAPDH mRNA levels, relative to the values in the mock set as 1. Values represent the mean ± standard deviation of triplicate samples. Reproducible results were obtained from two independent experiments. Mock: treated with Lipofectamine only; no treatment: no transfection.

Supplementary Figure S7. Inducing exon skipping by 9-mer LNA/DNA mixmer SSOs. Reporter cells were transfected with the indicated SSOs (30 nM) for 24 h. The levels of reporter minigene mRNA fragments were measured by RT-PCR and the signal intensity of each band was normalized according to its nucleotide composition. The exon skipping percentage was calculated as the amount of exon skipped transcript relative to the total amount of exon skipped and full-length transcripts. LNA

SSO (+10+24), which showed no exon skipping effects, was used as a control. Values represent the mean ± standard deviation of triplicate samples. Reproducible results were obtained from two independent experiments. The T_m of each SSO with a complementary RNA under low-sodium conditions is also shown. The data are the mean ± standard deviation (n = 4). Mock: treated with Lipofectamine only; no treatment: no transfection.

Supplementary Figure S8. 9-mer LNA SSOs induce exon skipping in a concentration-dependent manner. **(A-D)** RT-PCR analyses of RNA samples from reporter cells treated with the indicated SSOs at various concentrations for 24 h show the full-length upper band (587 bp) and the skipped lower band (466 bp). LNA SSO (+10+24), which showed no exon skipping effects, was used as a control. GAPDH was used as an internal control. **(E)** The signal intensity of each band was normalized according to its nucleotide composition. The exon skipping percentage was calculated as the amount of exon skipped transcript relative to the total amount of exon skipped and full-length transcripts. Values represent the mean ± standard deviation of triplicate samples. Reproducible results were obtained from two independent experiments. Mock: treated with Lipofectamine only; no treatment: no transfection.

Supplementary Figure S9. Exon skipping activity of short (6- to 9-mer) LNA SSOs. RT-PCR analyses of RNA samples from reporter cells treated with the indicated SSOs (30 nM) for 24 h. The signal intensity of each band was normalized according to its nucleotide composition. The exon skipping percentage was calculated as the amount of exon skipped transcript relative to the total amount of exon skipped and full-length transcripts. LNA SSO (+10+24), which showed no exon skipping effects, was used as a control. GAPDH was used as an internal control. Values represent the mean ± standard deviation of triplicate samples. Reproducible results were obtained from two independent experiments. The T_m of each SSO with a complementary RNA under low-sodium conditions is also shown. The data are the mean ± standard deviation (n = 3-4). Mock: treated with Lipofectamine only; no treatment: no transfection.

Supplementary Figure S10. Effect of mismatches on exon skipping activity and specificity. Reporter cells were transfected with the indicated SSOs (30 nM) for 24 h. The levels of reporter minigene mRNA fragments were measured by RT-PCR, and the signal intensity of each band was normalized according to its nucleotide composition. The exon skipping percentage was calculated as the amount of exon skipped transcript relative to the total amount of exon skipped and full-length transcripts. LNA SSO (+10+24), which showed no exon skipping effects, was used as a control. Values represent the mean ± standard deviation of triplicate samples. Reproducible results were obtained from two independent experiments. Mock: treated with Lipofectamine only; no treatment: no transfection.

Supplementary Figure S11. Quantitative analysis of competitive inhibition of 5' 6-FAM-labeled SSO duplex formation to the complementary RNA. Equal amount of a 5' 6-FAM-labeled SSO (A strand) and the complementary RNA (B strand) was mixed with various amount of an unlabeled competitor SSO (X strand) and annealed in 10 mM phosphate buffer (pH 7.2) containing 100 mM NaCl. After separation by 15% non-denaturing PAGE, the decrement of the fluorescence intensity that

corresponds to the amount of a labeled duplex (AB signal) with increasing free competitor SSO concentration [X] was curve fitted and half maximal inhibitory concentration of the competitor SSO (IC_{50}) was determined.

Supplementary Table S1.

Entry	ID	Sequence
1	-5+10	tCt tGa aGg cCt gTg
2	+10+24	aGt tTt cAa tTc cCt
3	+25+39	gAt tAc aGg tTc tTt
4	+40+54	cTc aAg aGt aCt cAt
5	+55+69	aAa tAt tCg tAc aGt
6	+70+84	aGg cTg cTc tGt cAg
7	+85+99	cTc tAg tCc tTc cAa
8	+100+114	cTc cTg gTa gAg tTt
9	+115-8	tCa aTt aCc tCt gGg

Supplementary Table S2.

Entry	ID	Sequence
1-1	-20-6	aAa tGa gAt gAa aAg
1-2	-17-3	gTg aAa tGa gAt gAa
1-3	-14+1	cCt gTg aAa tGa gAt
1-4	-11+4	aGg cCt gTg aAa tGa
1-5	-8+7	tGa aGg cCt gTg aAa
1	-5+10	tCt tGa aGg cCt gTg
1-6	-2+13	cCc tCt tGa aGg cCt
1-7	+2+16	aTt cCc tCt tGa aGg
1-8	+5+19	tCa aTt cCc tCt tGa
1-9	+8+22	tTt tCa aTt cCc tCt
6-1	+58+72	cAg aAa tAt tCg tAc
6-2	+61+75	tGt cAg aAa tAt tCg
6-3	+64+78	cTc tGt cAg aAa tAt
6-4	+67+81	cTg cTc tGt cAg aAa
6	+70+84	aGg cTg cTc tGt cAg
6-5	+73+87	cAa aGg cTg cTc tGt
6-6	+76+90	tTc cAa aGg cTg cTc
6-7	+79+93	tCc tTc cAa aGg cTg
6-8	+82+96	tAg tCc tTc cAa aGg
9-1	+103+117	gGg cTc cTg gTa gAg
9-2	+106+120	tCt gGg cTc cTg gTa
9-3	+109-2	aCc tCt gGg cTc cTg
9-4	+112-5	aTt aCc tCt gGg cTc
9	+115-8	tCa aTt aCc tCt gGg
9-5	+118-11	cAt tCa aTt aCc tCt
9-6	+121-14	cCa cAt tCa aTt aCc
9-7	-3-17	gTt cCa cAt tCa aTt
9-8	-6-20	aTa gTt cCa cAt tCa
9-9	-9-23	aTt aTa gTt cCa cAt

Supplementary Table S3.

Entry	ID	Sequence
1-6-1	-4+11	ctC ttG aaG gcC tgT
1-6-2	-3+12	Cct Ctt Gaa Ggc Ctg
1-6	-2+13	cCc tCt tGa aGg cCt
1-6-3	-1+14	tcC ctC ttG aaG gcC
1-6-4	+1+15	Ttc Cct Ctt Gaa Ggc
9-2-1	+104+118	tgG gcT ccT ggT agA
9-2-2	+105+119	Ctg Ggc Tcc Tgg Tag
9-2	+106+120	tCt gGg cTc cTg gTa
9-2-3	+107+121	ctC tgG gcT ccT ggT
9-2-4	+108-1	Cct Ctg Ggc Tcc Tgg

Supplementary Table S4.

Entry	ID	Sequence	T_m (°C) Low salt	T_m (°C) Medium salt
1	-1+14_15/15	TCC CTC TTG AAG GCC	>95.0	–
2	-1+14_8/15	TcC cTc TtG aAg GcC	82.6 ± 2.3	–
3	-1+14_7/15	tCc CtC tTg AaG gCc	84.6 ± 2.7	–
4	-1+14_5/15	tcC ctC ttG aaG gcC	69.5 ± 0.5	79.1 ± 0.2
5	-1+14_4/15	tcC ctC ttG aaG gcC	68.8 ± 2.6	74.8 ± 1.2
6	-1+14_3/15	tcC ctC ttG aaG gcC	62.1 ± 1.7	70.2 ± 1.2
7	-1+14_2/15	tcC ctC ttG aaG gcC	57.7 ± 2.1	66.1 ± 1.0
8	-1+14_1/15	tcC ctC ttG aaG gcC	55.1 ± 1.5	63.3 ± 0.2
9	-1+14_OMe	tcC ctC ttG aaG gcC	50.1 ± 1.8	58.4 ± 0.4
10	-1+14_DNA	tcc ctc ttg aag gcc	39.9 ± 1.3	52.2 ± 1.1

Supplementary Table S5.

Entry	ID	Sequence	T_m (°C)
1	+108-1_15/15	CCT CTG GGC TCC TGG	>95.0
2	+108-1_8/15	CcT cTg GgC tCc TgG	>88.0
3	+108-1_7/15	cCt CtG gGc TcC tGg	87.8 ± 0.6
4	+108-1_5/15	Cct Ctg Ggc Tcc Tgg	79.0 ± 1.9
5	+108-1_4/15	Cct Ctg Ggc Tcc Tgg	73.8 ± 0.8
6	+108-1_3/15	Cct Ctg Ggc Ucc Tgg	66.8 ± 0.4
7	+108-1_2/15	Cct Ctg Ggc Ucc Tgg	63.8 ± 1.0
8	+108-1_1/15	Cct Ctg Ggc Ucc Ugg	61.7 ± 0.2
9	+108-1_OMe	Cct Ctg Ggc Ucc Ugg	57.4 ± 0.8
10	+108-1_DNA	cct ctg ggc tcc tgg	53.0 ± 1.0

Supplementary Table S6.

Entry	ID	Sequence	T_m (°C)	$\Delta G°_{25}$ (kcal/mol)	K_d (M)
1	+114-1_4/9	cCt CtG gGc	66.7 ± 0.4	-20.7 ± 0.2	6.9×10^{-16}
2	+112-1_5/11	cCt CtG gGc Tc	75.8 ± 0.7	-23.9	3.2×10^{-18}
3	+110-1_6/13	cCt CtG gGc TcC t	83.3 ± 0.7	-27.2	1.2×10^{-20}
4	+108-1_7/15	cCt CtG gGc TcC tGg	87.8 ± 0.6	-29.2	3.7×10^{-22}
5	+106-1_8/17	cCt CtG gGc TcC tGg Ta	>88.0	-29.4	2.6×10^{-22}
6	+104-1_9/19	cCt CtG gGc TcC tGg TaG a	>88.0	-29.7	1.8×10^{-22}
7	+102-1_10/21	cCt CtG gGc TcC tGg TaG aGt	>88.0	-29.5	2.3×10^{-22}
8	+100-1_11/23	cCt CtG gGc TcC tGg TaG aGt Tt	>88.0	-30.0	1.1×10^{-22}

Supplementary Table S7.

Entry	ID	Sequence	T_m (°C)
1	+114-1_4/9	cCt CtG gGc	66.7 ± 0.4
2	+114-1_7/9_1	cCT CTG GGc	87.1 ± 1.9
3	+114-1_7/9_2	CCT CTG gGc	83.1 ± 2.7
4	+114-1_OMe	cCt CtG gGc	40.0 ± 1.0